



OPEN ACCESS

EDITED BY Frank J. M. Verstraete, University of California, Davis, United States

REVIEWED BY Boaz Arzi, University of California, Davis, United States Tanya C. Garcia University of California, Davis, United States David C. Hatcher, Consultant, Davis, CA, United State

*CORRESPONDENCE Silvio Kau, ⊠ silvio.kau@vetmeduni.ac.at

[†]These authors have contributed equally to this work and share first authorship

RECEIVED 28 June 2023 ACCEPTED 21 August 2023 PUBLISHED 20 September 2023

Sterkenburgh TR, Hartl B, Peham C, Nowak M, Kyllar M and Kau S (2023), Temporomandibular joint biomechanics and equine incisor occlusal plane maintenance. Front, Bioena, Biotechnol, 11:1249316. doi: 10.3389/fbioe.2023.1249316

COPYRIGHT

© 2023 Sterkenburgh, Hartl, Peham, Nowak, Kyllar and Kau. This is an openaccess article distributed under the terms of the Creative Commons Attribution License (CC BY). The use, distribution or reproduction in other forums is permitted, provided the original author(s) and the copyright owner(s) are credited and that the original publication in this journal is cited, in accordance with accepted academic practice. No use distribution or reproduction is permitted which does not comply with these terms.

Temporomandibular joint biomechanics and equine incisor occlusal plane maintenance

Tomas Rudolf Sterkenburgh 1,21, Bettina Hartl 31, Christian Peham 4, Michael Nowak⁵, Michal Kyllar³ and Silvio Kau³*

¹Polyclinic for Dental Preservation and Periodontology, University of Leipzig, Leipzig, Germany, ²Department of Industrial Engineering, Business Administration and Statistics, DEGIN Doctoral Program, Universidad Politécnica de Madrid, Madrid, Spain, ³Department of Pathobiology, Institute of Morphology, Vetmeduni Vienna, Vienna, Austria, ⁴Department of Companion Animals and Horses, Movement Science Group, University Clinic for Horses, Vetmeduni Vienna, Vienna, Austria, ⁵Veterinary Practice Dr. M. Nowak, Equine Clinic Meerbusch, Meerbusch, Germany

In equine dentistry, the physiological incisor occlusal surface is visually perceived as a plane with a distinct inclination to the head's coronal plane, extending rostroventrally to caudo-dorsally. To better understand the formation of this inclined plane and its connection to dental wear, we investigated the hypothesis that it arises from masticatory movements and the considerable distance between mandibular articular heads and the incisor occlusal surfaces, acting as the three points of support for the mandibles. Leveraging data from a large-scale clinical study involving static and dynamic orthodontic measurements in horses, we approximated the mandibular movement range where incisor occlusion and dental wear occur. By introducing and testing a segment coordinate system, we explored possible angular deviations from the occlusal plane caused by mandibular roll and pitch rotations during two lateral mandibular movement patterns, protrusion and retrusion. Theoretical biomechanical calculations and simulations confirmed the visual perception of the incisor occlusal surface as a plane. To further examine our assumptions, we employed a simple mechanical simulator to assess incisor normal occlusion and provoked malocclusions (diagonal, smile, and frown bite) by modifying temporomandibular joint (TMJ) movement patterns. The results from clinical investigations were corroborated by both the theoretical analysis and mechanical simulations, strengthening our understanding of the biomechanical basis behind the physiological incisor occlusal plane maintenance in horses. These findings have significant implications for equine dental health and contribute to a thorough understanding of TMJ dynamics.

KEYWORDS

equine dentistry, incisor occlusal surface, group function occlusion, dental wear, malocclusion, mastication, biomechanics

Introduction

Equine dental wear is caused by attrition (tooth-to-tooth contact) and abrasion (toothto-food contact) (Imfeld, 1996). This dental wear occurs due to compressive loading when two tooth areas are pressed against each other by masticatory muscle force and due to shearing loads when these tooth areas are moved over each other while maintaining chewing pressure. Occlusion has a decisive influence on dental wear; therefore, small deviations in

posture and occlusion can lead to chronic dental problems (Easley et al., 2011a; Taylor et al., 2018). Dental wear is influenced by extrinsic factors such as type of forage and abrasive particles in the food and intrinsic factors such as the hardness of the tooth structures and mastication biomechanics (Muylle et al., 1999).

In horses, chewing is a unilateral process that occurs on either the right or left side (Collinson, 1994; Tremaine, 1997; Baker and Easley, 2005; Staszyk et al., 2006a). The chewing cycle is described differently in the literature: during the opening stroke, the mandible moves ventrally (Bonin et al., 2006; Bonin et al., 2007; Simhofer et al., 2011), laterally either to the balancing (Bonin et al., 2006; Bonin et al., 2007; Sterkenburgh et al., 2022) or toward the working side (Bonin et al., 2006; Staszyk et al., 2022) and slightly rostrally (Simhofer et al., 2011; Staszyk et al., 2022) or caudally (Bonin et al., 2006; Bonin et al., 2007). The mandible either rotates around a vertical axis located symmetrically between the mandibular articular head (AH) of both sides (median axis) (Bonin et al., 2006) or it rotates around the AH of the working side mandible, while the AH of the balancing side slides in a rostral direction (Staszyk et al., 2022). A lateral movement may be superimposed. During the closing stroke, the mandible moves dorsally (Bonin et al., 2006; Bonin et al., 2007; Simhofer et al., 2011) until the mandibular cheek teeth of the working side contact those of the maxilla (Collinson, 1994; Tremaine, 1997; Baker and Easley, 2005). Furthermore, the mandible moves either rostrally (Bonin et al., 2006; Bonin et al., 2007) or caudally (Simhofer et al., 2011) and laterally to the working side (Bonin et al., 2006; Bonin et al., 2007; Sterkenburgh et al., 2022) during the closing stroke. The power stroke causes the mandibular cheek teeth to grind upon the maxillary teeth in a movement from ventral to dorsal and either in a medial (Tremaine, 1997; Bonin et al., 2006; Bonin et al., 2007; Sterkenburgh et al., 2022) or lateral (Simhofer et al., 2011) direction. Shortly before reaching the neutral position—at the point of maximum lateral displacement—the six mandibular and maxillary incisor teeth come into contact and masticatory pressure is carried by the incisor teeth and temporomandibular joints (TMJs). The contact between the incisor teeth at the end of each chewing cycle in the post-power "recovery" stroke is called incisor landing (Staszyk et al., 2022; Sterkenburgh et al., 2022). Throughout the chewing process, masticatory forces are distributed differently to the two TMJs, left and right maxillary and mandibular cheek tooth arcades, and mandibular and maxillary incisor teeth. The masticatory forces on the mandibular cheek teeth are highest during the power stroke, reaching up to 1956 N (Staszyk et al., 2006a; Huthmann et al., 2009). The bite force of the incisor teeth during food prehension is approximately 2% of body weight (Hongo and Akimoto, 2003). Chewing rates differ depending on forage, ranging between 68.5 and 83.9 chews/min (Weinert et al., 2020).

Occlusion of the incisor teeth is laterally restricted to the area between the two points of maximum lateral excursion to separation (LETS), also known as excursion to molar contact (EMC). In this area of incisor occlusion, masticatory pressure is mainly supported by the incisor teeth and the TMJs. To examine molar occlusion, the lateral excursion to molar contact test (LMC) is measured during equine dental examination (Limone et al., 2022). EMC ranges from 4.2 to 30 mm, with a mean of 11.7–12.3 mm and a median between 11 and 12 mm (Rucker, 2002; Rucker, 2004; Pimentel and Zoppa AL do, 2014). To identify LMC, the neutral position of the maxillary and mandibular

incisor teeth relative to each other is first determined with the mouth closed. From this position, the lower jaw is maximally deflected to the left and right, while the mouth remains closed. At the point of maximum deflection, the cheek tooth arcades come into contact and push the incisor teeth apart because of their angle (Rucker, 2004). The distance of the neutral position, respectively, to the right and left maximum deflection points with the jaws closed is called the left or right LETS (Easley et al., 2011b). Occlusal abnormalities in incisor teeth are common, and the reported numbers vary from 48.6% to 60% of the horses examined (Pimentel and Zoppa AL do, 2014; Kunz et al., 2020). Smile bite or ventral curvature (CV) of the incisor arcade, frown bite or dorsal curvature (CD), and incisor slant or diagonal incisor malocclusion (DIM) have been reported in 21.4%, 17.1%, and 27%–48.7% of examined horses, respectively (Pellachin, 2013; Kunz et al., 2020).

Accounting for all variables when simulating tooth wear *in vitro* is difficult (Lambrechts et al., 2006). Karme et al. (2016) used equine cheek teeth fixed in an artificial mastication apparatus to determine differences in microwear patterns using four different feeds. Sterkenburgh et al. (2022) performed computer simulations that mimicked cheek teeth wear using a simplified two-dimensional model. The stress and strain energies in the periodontal ligament and alveolar bone of equine incisor teeth were analyzed using finite element analysis (Schrock et al., 2013). To date, no study has investigated incisal wear in horses.

We hypothesized that the physiological occlusal surface of equine incisor teeth is planar. The starting point was the evidence-based knowledge about the masticatory process in horses. From the clinical orthodontic measurements, we derived insights on the potential TMJ dynamics required for maintaining the occlusal plane of the incisor teeth through theoretical geometric and biomechanical considerations. Furthermore, we utilized a mechanical mastication simulator to prove our theoretical considerations and demonstrated that incisor malocclusions such as DIM, smile bite, and frown bite may result from specific TMJ/mandibular movement patterns.

Materials and methods

Clinical assessment of static and dynamic orthodontic parameters

We analyzed the dental reports of 609 horses which have undergone a regular dental check (dental prophylaxis). The reports were collected by a single examiner (SK) over the period of April 2017 to September 2018 in Germany and Austria. The analyzed data included measurements of static and dynamic orthodontic parameters, i.e., horizontal overbite (also termed overjet (OJ)), horizontal underbite (also termed underjet (UJ)) and central incisor interdental space center offset (CO) at jaw symmetry position (static) and LETS (dynamic). Briefly, a detailed pre-treatment examination of the oral cavity was performed under sedation with 0.01 mg*kg-1 detomidine hydrochloride (Detogesic, Zoetis, Berlin, Germany) and 0.1 mg*kg-1 butorphanol (Torbugesic, Zoetis, Berlin, Germany). A dental holster (Pegasos4D, Waldkirch, Germany) was used to support the head during examination and orthodontic measurements. The head was elevated to a neutral position as previously outlined by Kau et al. (2020). Orthodontic measurements were performed using a stainless-steel

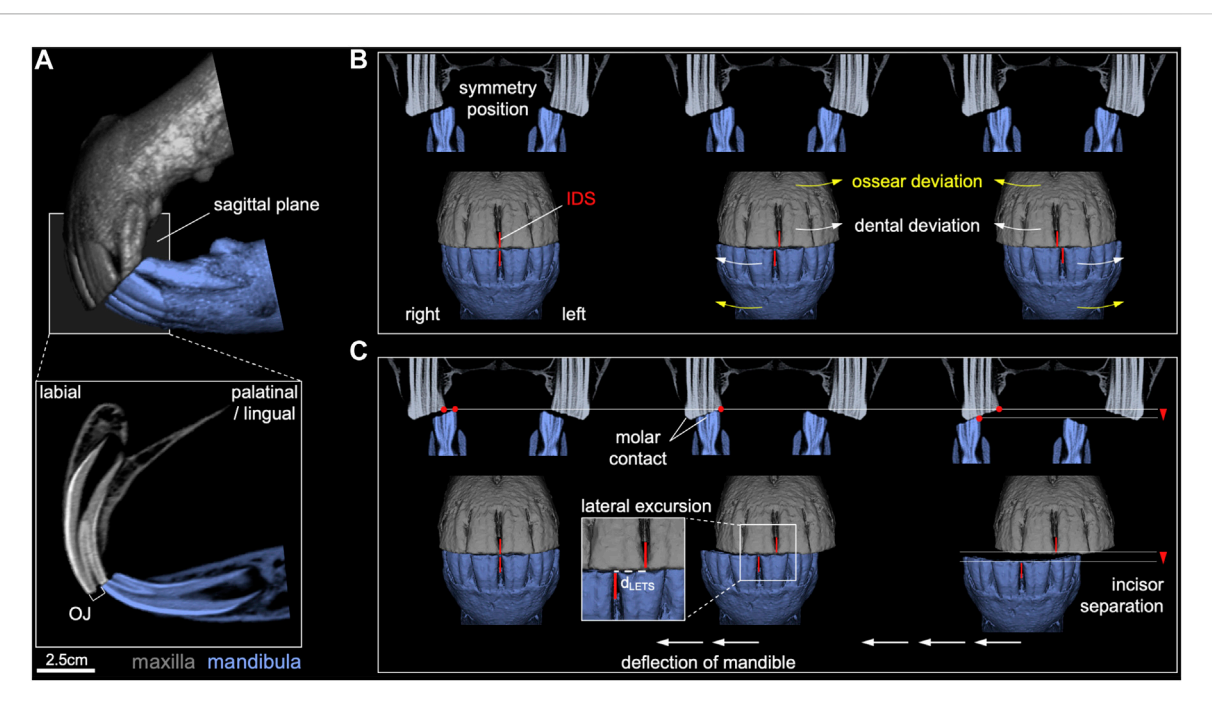


FIGURE 1
Graphical illustration of evaluated static and dynamic orthodontic parameters. (A) Overjet (OJ) for maxillary and mandibular central incisor horizontal occlusal plane discrepancy at the described head position. (B) Maxillary and mandibular central incisor interdental space (IDS) center offset. (C) Distance of mandibular lateral excursion to incisor separation (d_{LETS}) and molar contact.

length and angle measuring device (0-100 mm, Shinwa Rules, Niigata, Japan). OJ and UJ were measured as the distance between the mesiooccluso-labial edges of the maxillary and mandibular central incisor teeth (Figure 1A) (vertical deviation = 0 mm). This measure only considered horizontal over-/underbite with incisor teeth still in occlusion and occlusal planes oriented parallel. The center offset of the interdental spaces between maxillary and mandibular central incisor teeth was measured to assess functional asymmetry in the rostral dentition (Figure 1B), which was achieved by manually centering the maxillary and mandibular cheek teeth while visually controlling their alignment by deflecting the cheeks. The center offset distance to either side was considered the starting point for bilateral assessment of the incisor LETS (Figure 1C). Horses with a true vertical overbite or underbite, with maxillary and mandibular incisor's occlusal surfaces not in contact, or with marked incisor malocclusions were excluded from the study. The data analyzed in this study were limited to measurements obtained before the dental treatment.

Fundamentals and assumptions of mandibular and TMJ movement under incisor occlusion

During incisor occlusion, the mandible rests on three spatially separated areas, i.e., two TMJs and incisor occlusal surfaces. The mandible and consequently the incisor teeth undergo translatory movements of protrusion (forward) and retrusion (backward) under occlusion in a caudo-dorsal to rostro-ventral direction within the sagittal angle plane (SAP). This term indicates that the surface plane angulation can be measured in a sagittal plane (Listmann et al., 2017) (Figure 2A).

In the following text, the direction of mandibular protrusion under incisor occlusion was referred to as the "SAP+" direction and the corresponding retrusion direction as "SAP-". A movement perpendicular to the SAP is referred to as the "SAPL+" (directed rostro-dorsally) or as "SAPL-" (directed caudo-ventrally) (Figure 2A). Based on anatomical considerations, we assume a main protrusion movement of mandibular articular heads also largely along the SAP+ direction, but in a parallel articular head plane (AHP) (Figures 2A-C). Retrusion under incisor occlusion in the opposite direction (SAP-) is likely limited by the retroarticular process (RAP) (Figures 2A,B). For movements of the mandibular AH, we apply the terminology accordingly, as "AHP+," "AHP-," "AHP \perp +," and "AHP \perp -." With these designations, we transferred our considerations to the segment coordinate system of the incisor occlusal surface plane, thus avoiding imprecise combinations such as caudo-dorsal and rostro-ventral, in the following text. Lateral movements were referred to as "lateral".

From anatomical observations, it appears likely that the protrusion movement of the mandibular AHs under incisor occlusion goes mainly in the SAP+ direction with minor deviations. Figure 2C confines a range of assumed protrusion movements as an upward estimate of the directional deviation from this SAP+ movement direction and mark the vector components accordingly.

This section further outlined the biomechanical dimensions to evaluate and model the effect of TMJ dynamics and the resulting mandibular motion on incisor occlusal surface wear and maintenance of the occlusal surface as a plane. The assumed TMJ dynamics were deduced from observations of static and dynamic orthodontic measurements of mandibular motion reported in the literature, from own measurements, and from theoretical assumptions thereof that are drawn from this study.

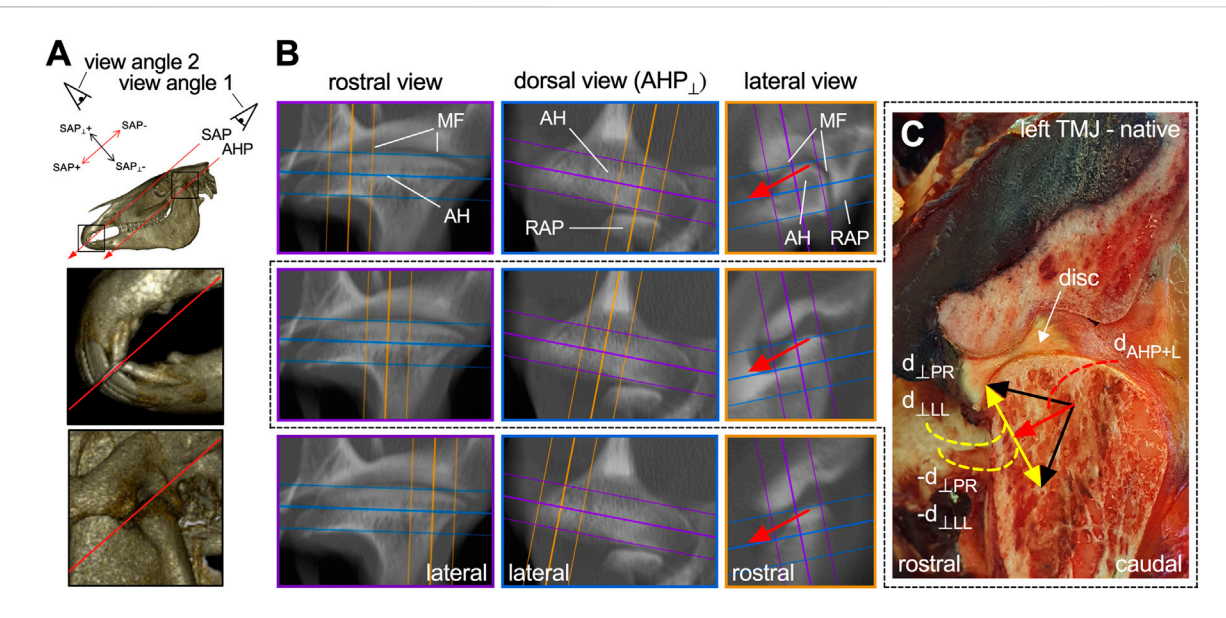


FIGURE 2
Multiple views of considered dentofacial planes and assumptive depiction of TMJ protrusion movement components. (A) Study view angle on the occlusal surface of incisor teeth sagittal angle plane (SAP) and mandibular articular head plane (AHP) in the TMJ. Image details point out SAP and AHP. (B) Multilevel multiplanar mean intensity projection reconstruction and native depiction of a left TMJ. Arrows indicate protrusion movement vectors. MF, mandibular fossa; AH, mandibular articular head; RAP, retroarticular process. (C) Native section at mid TMJ level; lateral view. Black arrows: Upward estimates of directional deviation with vector components in red and yellow. Vector naming as used for theoretical calculations, below (1 eq. perpendicular).

Mandibular range of motion under incisor occlusion

First, we determined the range of possible mandibular positions that would allow contact between the occlusal surfaces of the maxillary and mandibular incisor teeth and subsequent dental wear. This range primarily had a latero-lateral and SAP+ to SAP- direction as well as combinations of both and was estimated based on existing evidence and our own measurements during this study. LETS/EMC, often determined as part of standard dental care using the "lateral excursion test" (Figure 1C), describes the range of translational movement out of the symmetrical position of the mandible to the left and right while maintaining incisor occlusion. The magnitude of this displacement was reported in the literature as 1-30 mm with a mean average ($\pm SD$) of 12 ± 3.6 mm (Rucker, 2004; Pimentel and Zoppa AL do, 2014; DeLorey, 2007; Carmalt et al., 2003), and we also additionally evaluated this in our study. An SAP+ and SAP- translational jaw movements (i.e., protrusion and retrusion under incisor occlusion) changed dynamically during mastication and passively changes with different head positions (Griffin, 2013). The total magnitude for this displacement during mastication was given in the literature as 5-18 mm in adult horses and 3-4 mm in foals. Considering the reported values, the mean average (±SD) in adult horses was 8.8 ± 2.2 mm (Bonin et al., 2007; Simhofer et al., 2011). SAP+ and SAP- mandibular movement, however, can be influenced by cheek tooth pathologies, dental treatment, and feed consistency (Simhofer et al., 2011; Carmalt et al., 2003). The proportion of masticatory SAP+ and SAP- jaw movement under incisor occlusion can only be assumed. We measured the central OJ and UJ with an elevated head position, suggesting that a more orthognathic and full occlusion superimposed antagonistic incisor teeth with a lowered head. The latter occurs naturally during grazing and feeding. Regardless of the rostro-caudal mandibular displacement that occurs, it can be stated based on geometric considerations that incisor occlusion ends when the mandibular arcade is displaced in SAP+ or SAP- direction until the occlusal surfaces are no longer in contact. We also assumed that during jaw deflection under incisor occlusion, there may be minimal mandibular pitch and a roll around a latero-lateral and SAP "in-plane" axis, respectively. Since incisor occlusion may involve various directions of jaw movement, a comprehensive understanding of these movements, including translation to the TMJs, will aid in understanding equine incisor wear and occlusal plane maintenance.

Movement pattern of the TMJs under incisor occlusion

Based on possible mandibular movements under incisor occlusion, the corresponding movement dynamics of the TMJs can be approximated and modeled accordingly. Due to the rigid bony mandible, any movement of the occlusal surface of the mandibular incisor teeth, whether rotatory or translatory, is transferred to the corresponding TMJs. Protrusion (SAP+) and retrusion (SAP-) translatory movements result in a corresponding AHP+ and AHP- movements of both mandibular AHs in the TMJs (Figures 3A,B). In horses, latero-lateral mandibular incisor movements are described as the rotation of the mandible around an axis, directed from SAP \perp + to SAP \perp -, i.e., perpendicular to the SAP plane. Two rotational movement patterns are differentiated:

 First, resulting from a rotation of the mandible around a virtual axis located symmetrically between the two mandibular AHs. This causes the working-side AH to move backward and the balancing-side AH to move forward on a circular path

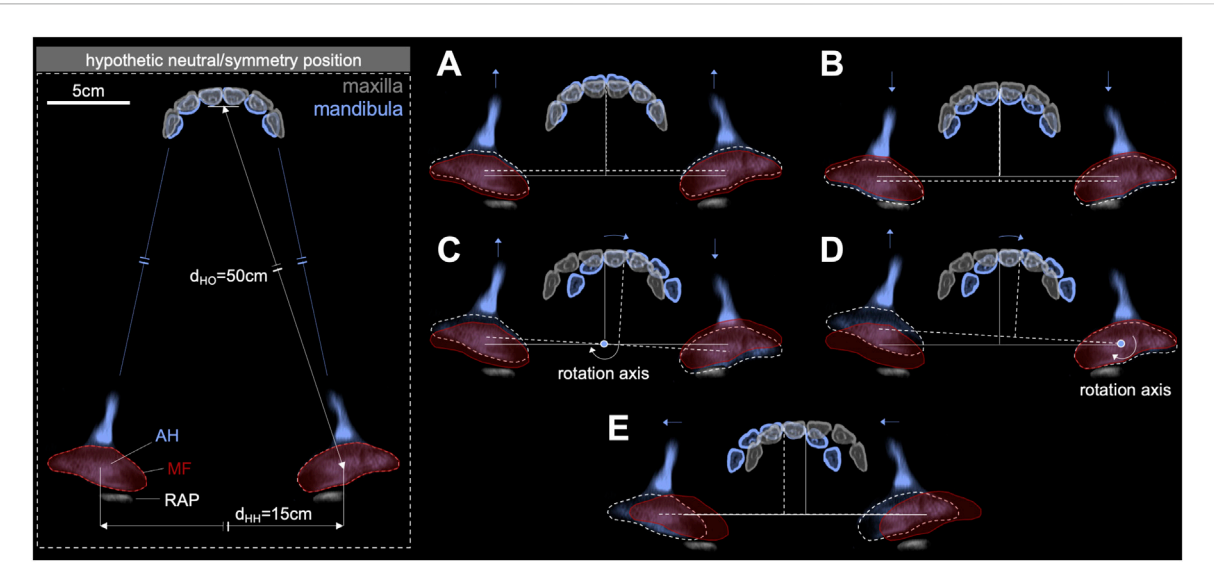


FIGURE 3

TMJ movements under incisor occlusion. (A) Protrusion (SAP+) and (B) retrusion (SAP-) range, (C) laterotrusion movement around an interarticular rotation axis along SAP $_{\perp}$ + to SAP $_{\perp}$ - (pattern no. 1), (D) laterotrusion movement around a mandibular articular head rotation axis along SAP $_{\perp}$ + to SAP $_{\perp}$ - (pattern no. 2), and (E) latero-lateral translatory mandibular movement (side shift). AH, mandibular articular head; MF, mandibular fossa; RAP, retroarticular process.

around the interarticular axis of rotation (Figure 3C) (Bonin et al., 2006). It is further referred to as movement pattern no. 1.

• Second, based on anatomical boundaries and prior research on non-midline jaw movements and associated TMJ dynamics in humans, we further propose and theoretically model an alternative rotation around an axis via the AH on the working side, while the AH on the balancing side slides off in an AHP + direction (Figure 3D). It is further referred to as pattern no. 2. In humans, this type of movement is described as both rotation around and translation along a virtual helical axis (Koolstra, 2002). Staszyk et al. (2022) suggested this type of movement in horses; however, this has not been validated yet.

Using our mechanical simulator, combinations of the previously described TMJ motion patterns were simulated and checked for their impact on the incisor occlusal surface plane maintenance.

Additionally, in humans, the lateral movement of the mandibular incisor teeth involves not only the rotation of the mandible around the working-side AH but also a lateral translatory component, that can occur progressively (Bennett movement) or spontaneously (immediate side-shift). This movement displaces the entire mandible toward the working side (Bennett, 1908; Preiskel and Goldstein, 2021). In our study, we also considered that this type of TMJ movement occurs in horses (Figure 3E), but do not use it in simulator experiments.

Calculations

After considering all the movement patterns, we quantified the extent and possibility of each movement. By performing geometrical calculations, we aimed to provide a theoretical estimate of the impact of each of the five movement patterns in Figure 3 on the occlusal

surface of incisor teeth. These calculations served to understand and further model the mechanics of jaw movement and its effects on the occlusal surfaces of the incisor teeth.

For our theoretical considerations, we assumed two horse heads. First, a male 12-year-old Warmblood horse (WBL) with a distance of $d_{\rm HO}$ = 50 cm between the mandibular AHs and central incisor's occlusal surface and a distance of $d_{\rm HH}$ = 15 cm between the AHs (interarticular distance), as shown in Figure 3. Second, a pony head was considered, being $d_{\rm HO}$ = 29.1 cm and $d_{\rm HH}$ = 9.7 cm. These values are derived from computed tomography (Warmblood) and skull (pony) measurements.

A) LETS of incisor teeth

First, the pivot point distance of pattern no. 1 to the incisor occlusal surface d_{BO} (Figure 4A) was calculated using the Pythagorean theorem as follows:

$$d_{BO} = \sqrt{d_{HO}^2 - \frac{d_{HH}^2}{4}}. (1)$$

Owing to the rotational movement, the lateral excursion represented a circle segment. With a small angle of rotation and a large distance between the center of rotation and incisor teeth in horses, a linear distance can be inferred. This corresponds to the length of the circular segment in a good approximation, which was followed in this study.

For pattern no. 1, the distance covered by the left (L) mandibular AH in AHP+ direction $d_{AHP+L}^{No.1}$ and the distance covered by the right (R) AH in AHP- direction $d_{AHP-R}^{No.1}$ are in correspondence to the lateral excursion d_{LETS} of the six incisor teeth according to the theorem of intercept. d_{LETS} , and the AH movement and the lateral excursion are related to each other via the length of the rotation arms:

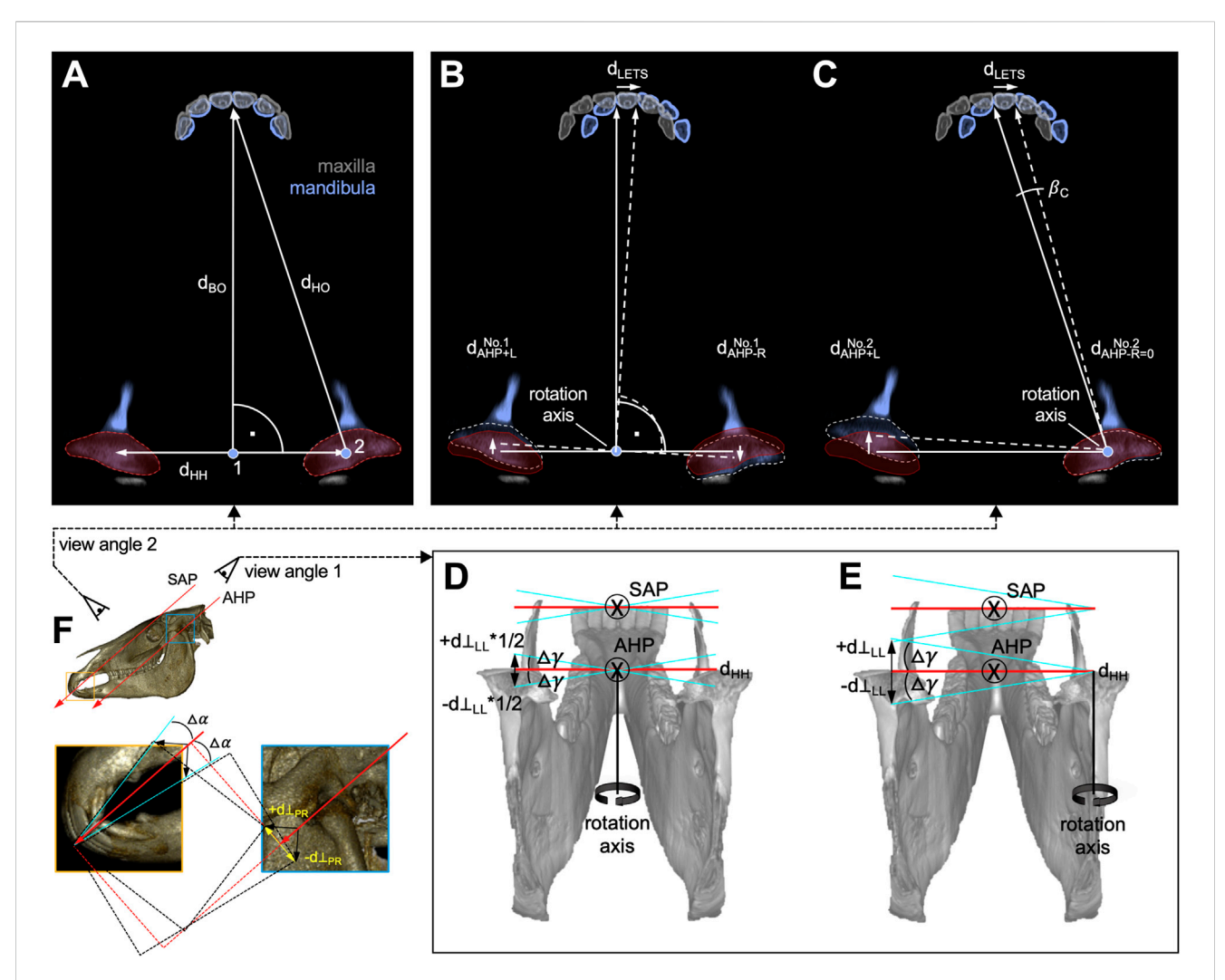


FIGURE 4

View on mandibular articular heads (AHs) and incisor teeth with distances, angles, and rotation axes in laterotrusion (**A–E**) and protrusion/retrusion (**F**) movement. (**A**) Neutral/symmetry position; 1, interarticular and 2, right AH SAP $_{\perp}$ rotation axis. (**B, C**) Incisor and TMJ movements integrating rotation pattern no. 1 and no. 2. d_{BO}, distance between interarticular "Bonin" pivot point and incisor occlusal surface; d_{HO}, distance from AH to incisor occlusal surface; d_{CC}, interarticular distance; d_{LETS}, LETS distance; d_{AHP $_{\perp}$} and d^{No2}_{AHP $_{\perp}$} left AH movement distances; d^{No1}_{AHP $_{\perp}$}, right AH caudal movement distance. (**D**) the perpendicular movement component d_{LLL} causes a roll around the SAP+ axis of Δ Y. (**E**) For pattern no. 2, the perpendicular movement components are opposing + d_{LLL}*1/2 and -d_{LLL}*1/2. (**F**) Considerations to mandibular/incisor occlusal plane rotation (pitch) due to protrusion. No angular deviation occurred if the AH movement was parallel to the SAP+ direction (red arrows). A perpendicular movement component d_{LPR} caused a Δ α angle variance. The black arrows are upward estimates of the directional variances. SAP+, incisor occlusal surface protrusion direction; AHP + assumed AH plane protrusion direction.

$$d_{AHP+L}^{No.1} = -d_{AHP-R}^{No.1} = \frac{d_{HH}/2}{d_{BO}} * d_{LETS}.$$
 (2)

For the alternative movement pattern no. 2, the AH of the right side has no translatory movement component, i.e., $d_{AHP-R}^{No.2}=0$, while $d_{AHP+L}^{No.2}$ then results as follows:

$$d_{AHP+L}^{No.2} = \frac{d_{HH}}{d_{HO}} d_{LETS} \sim 2^* d_{AHP+L}^{No.1}$$
with $d_{HO} \sim d_{BO}$ (3)

To calculate the angular deviation from the occlusal plane in the incisor teeth based on distances, the possible rotation (roll) of the mandible (Figures 4D,E), occurring in connection with these

movements, patterns was determined. If the rotation axis is perpendicular to SAP, no roll occurs. A motion component leaving this plane, however, will result in a deviation from the occlusal plane. The extent of the rotation is indicated by the motion component $d_{\rm LLL}$ perpendicular to the plane in SAP $_{\rm L}+$ or SAP $_{\rm L}-$ directions. Only if $d_{\rm LLL}\neq 0$, the latero-lateral motion was associated with roll and thus results an angular change.

Based on our anatomical observations, we assumed that both mandibular AH movement patterns no. 1 and no. 2 largely occurred in the described AHP plane.

For upward estimation of a maximum angle of rotation for movement pattern no. 2, we assumed a perpendicular movement component $d_{\perp LL}$ of the same size as $d_{AHP-R}^{No.2}$, respectively, occurring

perpendicular to the plane. This acted on the distance between the AHs (d_{HH}) and produced a rotation (roll) of

$$\Delta y = \operatorname{atan}\left(\frac{\mathbf{d}_{\perp LL}}{d_{HH}}\right) = \operatorname{atan}\left(\frac{\mathbf{d}_{AHP+L}}{d_{HH}}\right),$$
 (4)

as described in Figure 4E. For movement pattern no. 1 (Figure 4D), we assumed an opposing $1/2d_{\perp LL}$ acting on $1/2d_{HH}$, which leads to the same $\Delta \gamma$.

For a better comprehension of the angular deviation $\Delta \gamma$, which is due to lower jaw rolling motions, we look at the skull along the SAP+ and AHP+ axes with the eye position as marked in Figure 4F. This perspective is unusual but allows easier explanation of angular deviations (Figures 4D,E).

B) Protrusion under incisor occlusion

While excessive mandibular backward movement in AHP– direction is limited, forward movement at the level of incisor occlusal surfaces occurred along the occlusal surface plane in the SAP+ direction. The concomitant mandibular AH movement is in a similar direction (AHP+), however, followed AH mobility given by TMJ anatomy (Figures 2B,C). The different AH plane angles may have resulted from the shape of the articular surfaces. Angle variances may therefore lead to mandibular rotation (pitch) around the latero-lateral axis.

As an upward estimate in mandibular incisor forward movement (protrusion), we considered both mandibular AHs to have the same perpendicular movement component $d_{\perp PR}$ in the SAP $_{\perp}$ + or SAP $_{\perp}$ - directions. This results in an upward estimate for the deviation from the SAP+ direction as shown in Figure 4F. The angular change $\Delta\alpha$ due to this movement was calculated as follows:

$$\Delta \alpha = \operatorname{atan}\left(\frac{\mathbf{d}_{\perp PR}}{\mathbf{d}_{BO}}\right). \tag{5}$$

C) Lateral translatory mandibular excursion (immediate side shift)

During a lateral translatory movement of the entire mandible, it is to be expected that both AHs of the mandible show a movement component perpendicular to the incisor occlusal plane. Following the articular bone structure, the right and left perpendicular movement components likely not oppose but aim in SAPL— direction and differ in size. This would lead to mandibular roll, although there is no evidence that this translatory movement exists in horses.

Mechanical simulation of TMJ movement and incisor occlusal surface wear

To examine the shaping of the incisor occlusal surface in relation to TMJ movements, we designed and constructed a simple mechanical simulator system (Figure 5A). The six incisor teeth were represented by chalk bars with cuboid shape and a latero-lateral width of approximately 4.75 cm, an SAP+/– extension of approximately 2.0 cm, and a low abrasion resistance. Simulator dimensions were determined to closely mimic those of the pony head used in our theoretical calculations ($d_{\rm HH}=9.7$ cm and $d_{\rm HO}=29.1$ cm). The TMJs

were represented by two adjustable servo motors. As control we used an Arduino nano board (Arduino S.r.l., Italy). Rather than transferring mandibular movement to the TMJs, we emulated the assumed range of TMJ motion by designating the servomotors as the point of mandibular movement initiation. The rostro-caudal movement range of the left servomotor is illustrated in Figure 5B. Simplifying the simulator design, a mandible was rigidly connected to the test table with the upper jaw moving. To perceive the upper jaw as stationary, while the mandible moves as expected, it is necessary to move with the maxillary subordinate reference frame. The reference frame choice does not affect the results of the abrasive occlusal wear experiment. The simulator system enables mimicking TMJ movements, which in turn facilitates induction of corresponding movement patterns in the mandible during incisor occlusion (Figures 5C,D). We simulated various movement patterns, utilizing parameter sets determined in the clinical assessment. The servomotor settings are

The total number of movements was performed in 500 cycles, each consisting of 20 latero-lateral and four protrusion–retrusion movements. Values were adapted to the range of own measurements in smaller horses and theoretical assumptions.

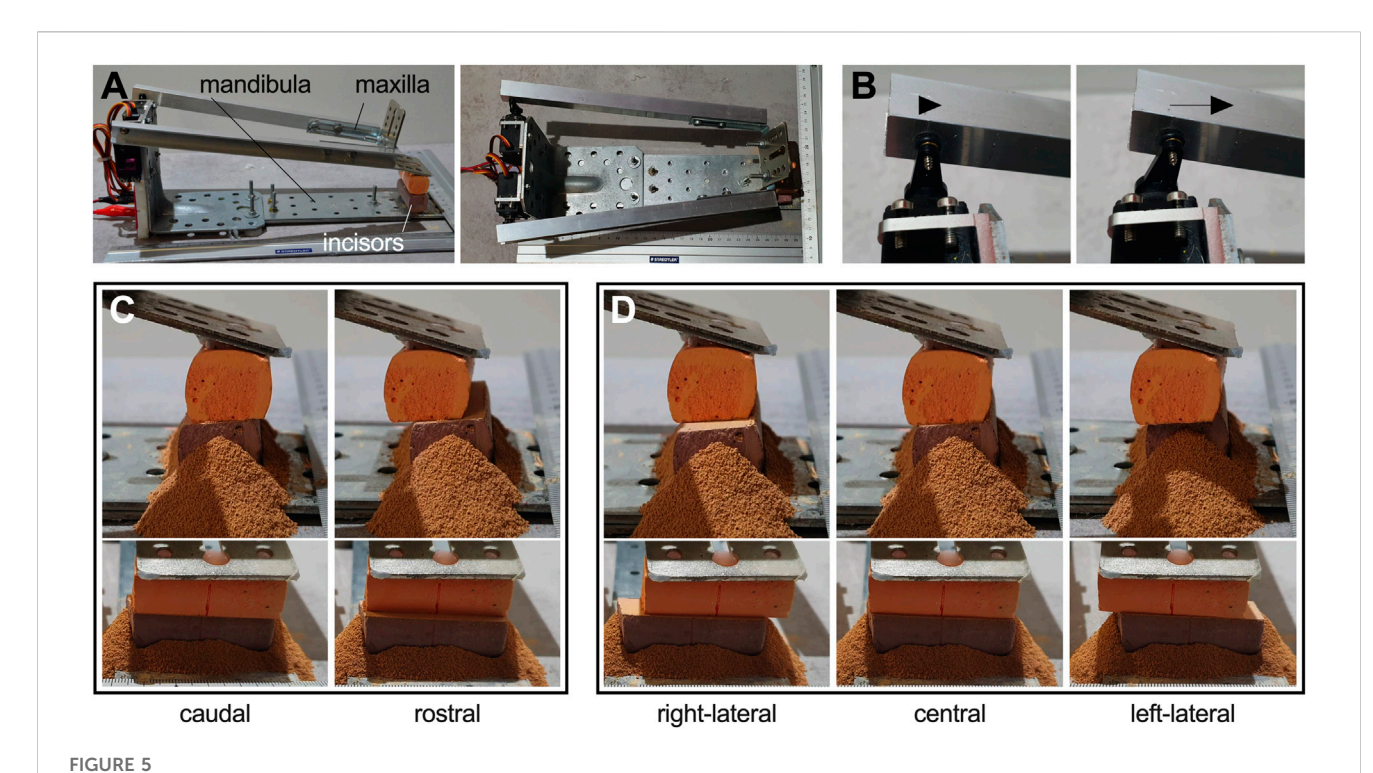
Data analysis and statistics

Data were analyzed using a combination of descriptive and inferential statistics. For the descriptive data analysis, measures of central tendency (i.e., mean and median) and measures of variability (i.e., standard deviation and range) were calculated for the variables of interest. We then performed normality distribution testing using a Shapiro-Wilk test to determine appropriateness using parametric tests. We also checked for outliers using the ROUT test (Q: 0.1%). The specific inferential tests used for each analysis and their outputs are described in the respective text passage or Figure caption. In addition, we performed simple linear regression analysis to examine the strength and direction of the relationship between pairs of continuous variables (age vs. OJ/CO/LE right/LE left). We used the least squares method to estimate the regression coefficients and the coefficient of determination to assess goodness of fit. The statistical significance of regression coefficients was tested using a t-distribution with a significance level of 0.05, which was used for all hypothesis testing in this study. All statistical analyses were conducted using the GraphPad Prism software package (GraphPad Software, SD, USA).

Results

Orthodontic measurements add to current evidence and infer no marked age dependency

To better approximate the range of motion that mandible and mandibular AHs in the TMJs have under incisor occlusion, we evaluated pre-treatment static and dynamic orthodontic measurements in a cohort of mainly large horses (88.2%) from South Germany. In total, data of 609 horses with a mean age (±SD)



Mechanical simulator setup. (A) side view (left); top view (right). (B) example for a servo range of motion. (C and D) mandibular movement: (C) SAP- retrusion (left) and SAP+ protrusion (right). (D) Lateral movement from right excursion of the mandibular arcade over the neutral position to left excursion. (C and D) Upper panel: side view; lower panel: frontal view of the same situation. Powdery abrasion is visible around the lower arcade.

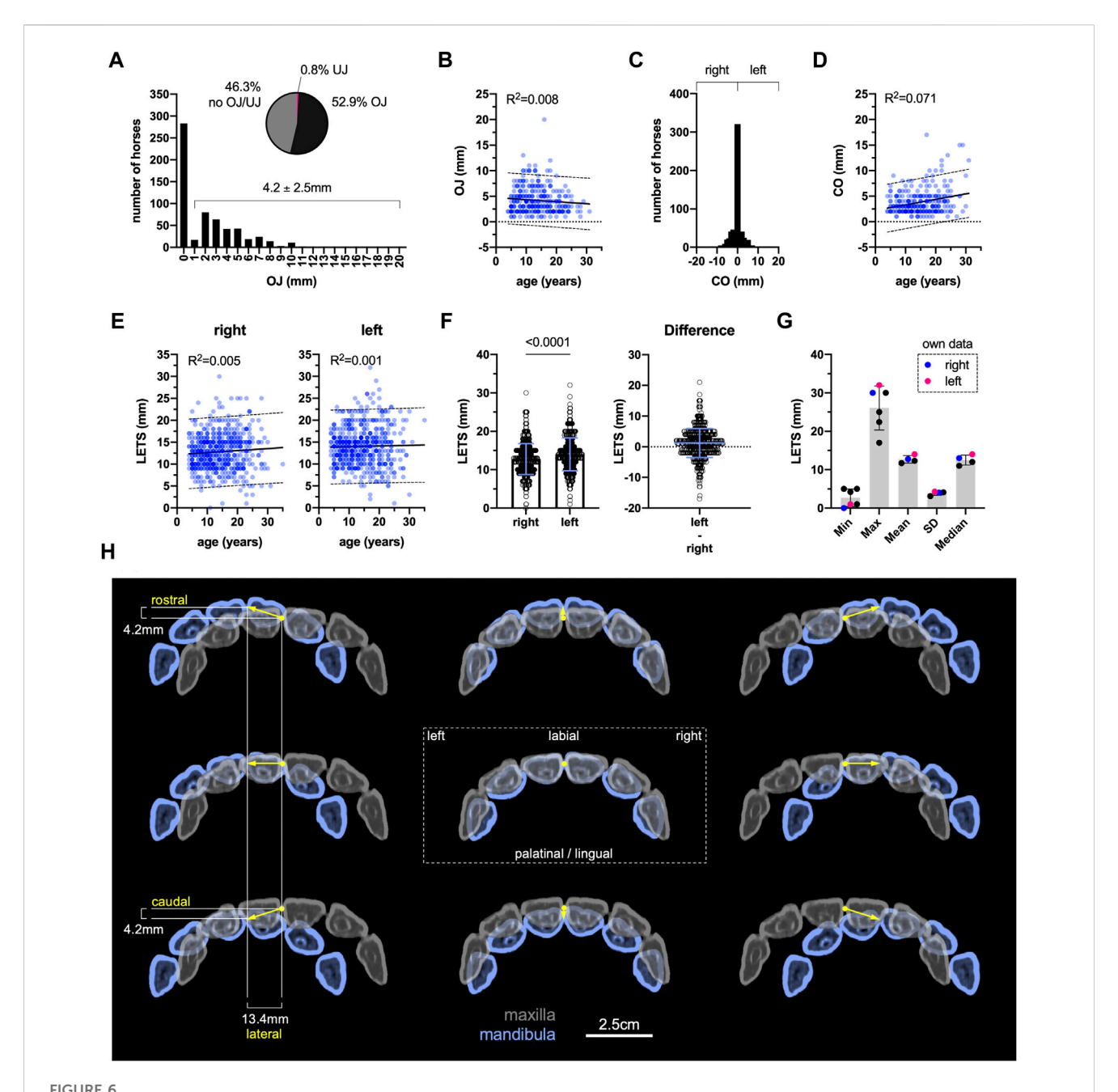
TABLE 1 Tested servo motor settings to mimic TMJ movements under incisor occlusion.

| Movement pattern | Assumed occlusal plane shape | Type of occlusion | SAP movement direction | Servo settings for mandibular movement | |
|---|------------------------------|-------------------|---------------------------|---|-----------------------|
| | | | | Laterotrusion | Protrusion-retrusion |
| No. 1 (Figure 4B) symmetric to both sides | Even plane | Normocclusion | SAP+ to SAP- | ±0.75 mm opposite | ±1.5 mm simultaneous |
| | | | SAP⊥+ to SAP⊥- | <0.5 mm opposite | <0.75 mm simultaneous |
| No. 1 (Figure 4B) asymmetric to one side | Diagonal even plane | Malocclusion | SAP+ to SAP- | ±1.0 mm opposite | ±1.5 mm simultaneous |
| | | | SAP⊥+ to SAP⊥- | <1.0 mm opposite | <0.75 mm simultaneous |
| No. 2 (Figure 4C) symmetric to both sides | Even plane | Normocclusion | SAP+ to SAP- | ±1.5 mm while other servo in rest and <i>vice versa</i> | ±1.5 mm simultaneous |
| | | | SAP⊥+ to SAP⊥- | <0.75 mm for servo in motion | <0.75 mm simultaneous |
| No. 2 (Figure 4C) asymmetric to one side | Diagonal even plane | Malocclusion | SAP+ to SAP- | ±2.0 mm while other servo in rest | ±1.5 mm simultaneous |
| | | | SAP⊥+ to SAP⊥- | <0.5 mm for servo in motion | <0.75 mm simultaneous |
| No. 3 | Smile | Malocclusion | SAP+ to SAP- | <1.0 mm opposite | ±1.0 mm simultaneous |
| | | | SAP⊥+ to SAP⊥- | +/- 7.0 mm opposite | ±7.0 mm simultaneous |
| No. 4 | Frown | Malocclusion | SAP+ to SAP- | <1.0 mm opposite | ±1.0 mm simultaneous |
| | | | SAP⊥+ to SAP⊥- | -/+ 7.0 mm opposite | ±7.0 mm simultaneous |

SAP, sagittal angle plane.

of 14 ± 6.2 years and age range from 4 to 35 years were included. In the investigated head position, OJ was the most common occlusal deviation among the horses with horizontal protrusion or retrusion of mandibular incisor teeth (Figure 6A). The population-wide mean

OJ (\pm SD) of 2.2 \pm 2.8 mm (range: 0–20 mm) excelled the extent of a mean UJ (\pm SD) of 0.02 \pm 0.2 mm (range: 0–3 mm) both in amplitude and variation. In the underrepresented proportion of small horses (Islandic and Connemara; n=55), mean OJ was



Evaluation of static and dynamic orthodontic parameters. (A) Overjet (OJ)/underjet absolute and relative distribution, n = 609. (B) Linear regression analysis OJ vs. age, F = 2.69, p = 0.102, n = 322. (C) Central incisor interdental space center offset (CO) frequency distribution and (D) linear regression analysis OC vs. age, F = 21.68, P = 0.0001, P

 1.5 ± 2.2 mm (range: 0–10 mm), whereas UJ was not represented. In ponies (Shetland; n=17), the mean OJ was 0.5 ± 1.7 mm (range: 0–7 mm), and mean UJ was 0.2 ± 0.7 mm (range: 0–3 mm). Considering only horses with OJ or UJ revealed values of 4.2 ± 2.5 mm and 2.4 ± 0.5 mm, respectively. The extent of an OJ seems not to change with an increase in age (Figure 6B).

After manual centering of the cheek teeth to symmetric position, maxillary and mandibular central incisor interdental spaces (IDS)

were either located one above the other or slightly deviated to either side in most horses. A marked center offset (CO) was only observed in few horses (Figure 6C). In case of a center offset (47.3%), there was no difference between left (3.8 \pm 2.7 mm) and right (3.9 \pm 2.4 mm), p=0.327, Mann–Whitney U test. A low proportion of variation in center offset measures can be explained by the age of horses examined, representing a weak positive association (Figure 6D).

Lateral excursion to incisor separation (LETS) to either side appears even less related to age (Figure 6E). Although mean (\pm SD) lateral excursion to the right (12.8 \pm 4.0 mm) appeared significantly smaller than to the left (14.0 \pm 4.3 mm), the overall mean difference was yet very low (Figure 6F). Comparing our overall results on lateral excursion with the values reported in the previously published literature, data are in good agreement (Figure 6G). In a small number of horses, lateral excursion to the right was 11.8 \pm 4.2 mm, and that to the left was 13.2 \pm 4.4 mm (range: 1–24 mm). In ponies, lateral excursion to the right and left was 8.6 \pm 1.9 mm and 9.9 \pm 2.8 mm, respectively (range: 4–15 mm).

These findings helped in the theoretical analyses of mandibular and TMJ angular changes and in biomechanical simulations under incisor occlusion. Figure 6H illustrates how mean overall values relate to the superposition of maxillary and mandibular six incisor teeth upon associated mandibular and TMJ movements under incisor occlusion.

Low mandibular pitch and roll helps maintain incisor occlusal surfaces as a plane

Based on our theoretical depiction of TMJ and corresponding mandibular movement patterns during incisor occlusion, we computed the occurrence and degree of mandibular rotation $\Delta\alpha$ along a latero-lateral axis (pitch) and $\Delta\gamma$ along the SAP+/– axis (roll). This analysis helped inferring a potential dynamic tilt of the incisor occlusal surface plane during TMJ movements under incisor occlusion. The calculations were executed for all TMJ movement patterns described (Figures 3A–E), embracing dimensions of the two horse head examples (WBL/pony).

While clinical orthodontic measurements in horses with OJ and UJ showed an average approximation to protrusion and retrusion jaw mobility of 4.2 mm and −2.4 mm respectively, we theoretically simulated these population values (mainly large horses) as the potential maximum mobility occurring in ponies. In the WBL example, we upward considered a maximum protrusion of 10 mm. Essentially, we assumed that the range of motion in our example was at the upper limit of what could be expected, while still maintaining some degree of incisor occlusal contact. Substituting $d_{\perp PR} = 10 \text{ mm}$ and $d_{BO} = 494 \text{ mm}$ for the WBL into Equation (5) yielded a mandibular roll of $\Delta \alpha \approx 1.16$ angle deg. Embracing orthodontic OJ data and pony head dimensions of our simulator resulted in a $\Delta\alpha$ < 0.82 angle deg. A d_{LPR} = 10 mm and used pony head dimensions yield a slightly higher $\Delta \alpha$ of \cong 2.0 angle deg. Computed angular deviations are alike considered not to interfere with the perception of the incisor occlusal surface as a plane.

In laterotrusion computations, movement pattern no. 1 yielded a slightly higher mandibular pitch as pattern no. 2, with a small $\Delta \gamma$ difference of 0.02 angle deg. for both the WBL and pony head (Table 2).

Based on anatomical observations, we anticipated an immediate side shift that would involve both lateral mandibular articular head movements to be accomplished by movement components of the mandibular AHs in the same SAP \perp - direction, but of different magnitude. The angular difference $\triangle \alpha$ will be of similar magnitude to $\triangle \alpha$ from protrusion/retrusion movement computations, while $\triangle \gamma$ only occurs due to the difference in magnitude of equilateral

SAP \perp - movement components and thus will be markedly smaller than calculated for the two rotative laterotrusion patterns.

Simulator results confirm the normal perception of incisor occlusal surfaces as a level plane

In light of the outlined theoretical considerations, we conducted mechanical simulations of masticatory movements under incisor occlusion and analyzed the differences between various movement patterns. The results were derived after 10 k latero-lateral and 2 k retrusion–protrusion movement cycles. With reference to mean annual wear across central to corner incisor teeth in wild equids (Smuts, 1974) and what is known from domestic equine cheek teeth (Staszyk et al., 2006b; Dixon et al., 2011), we assumed an incisor wear of 2 mm/year and 1 chewing cycle per second. This led to the following: 1 cycle/sec * 3.6 k sec/h * 5 h/d * 365 days/y = 3.3 million cycles/mm in a living horse. The wear on the chalk bars in our simulator setup was around 5 mm per 10 k + 2 k cycles. Each wear simulation thus equals 2.5 years in a real horse, whereas one cycle in the simulator corresponds to 275 cycles in a living horse.

Servo settings simulating the lateral jaw excursion equally with pattern no. 1 (Figure 7A), and no. 2 (Figure 7B), resulted in a flat appearance of the contact surface between chalk bars, which closely resembled the incisor occlusal surface plane in this model. For both movement patterns, the chalk bars exhibited a predominant laterolateral surface wear pattern (Figures 7C,D).

Asymmetric latero-lateral mandibular AH movements lead to diagonal incisor malocclusion

The TMJ movement background of diagonal incisor malocclusion (DIM) development was tested transferring theoretically derived information on altered mandibular AH movements to the mechanical simulator. Servo settings were changed to run asymmetric lateral jaw excursion to the left, which was limited by the left LETS and by the symmetry position. We performed this for motion pattern no. 1 and no. 2, starting with a level plane parallel to the ground, and both simulations resulted in a flat but diagonally inclined contact surface between chalk bars (Figures 8A,B).

Simulation of more complex patterns no. 3 and no. 4 induce smile and frown malocclusion

On the basis of laterotrusion pattern no. 1, we tested a situation where the two mandibular AH movements in SAP+ and SAP- direction are small but combined them with a large difference in left and right SAP⊥ movement components. This resulted in a pronounced mandibular roll around the SAP+/- axis with increasing excursion. Depending on whether this roll occurred in the same or in the opposite direction to the latero-lateral deflection of the mandible, a smile or frown was observed, respectively (Figures 8C,D).

TABLE 2 Head dimensions and calculation results in laterotrusion jaw movement.

| Data | source | Variable | WBL | Pony |
|----------------------|------------------------|-------------------------------|----------|----------|
| Clinical measurement | | d_{LETS} | 13.4 mm | 9.25 mm |
| | | d _{HH} | 150 mm | 97 mm |
| | | d _{HO} | 500 mm | 291 mm |
| | | d_{BO} | 494 mm | 287 mm |
| Calculation results | Movement pattern no. 1 | $\mathrm{d}_{\mathrm{AHP+L}}$ | 2.03 mm | 1.56 mm |
| | | d_{AHP-R} | -2.03 mm | -1.56 mm |
| | | Δγ | 1.55 deg | 1.84 deg |
| | Movement pattern no. 2 | d_{AHP+L} | 4.02 mm | 3.08 mm |
| | | d_{AHP-R} | 0.00 mm | 0.00 mm |
| | | Δγ | 1.53 deg | 1.82 deg |



FIGURE 7
Simulation results covering symmetric latero-lateral movement patterns. Movement pattern no. 2 (A) and movement pattern no. 1 (B) both educed a flat surface plane. (C, D) Detail view on the chalk surface wear pattern.

Discussion

The objective of our research was to examine the dynamic shaping of incisor occlusal surfaces in the horse. We focused on TMJ movements occurring during incisor occlusion and what influence different motion patterns have in normal incisor occlusion and malocclusion. To achieve this, we conducted clinical studies to assess the population-wide range of orthodontic parameters, including mandibular motion during incisor occlusion. Using these results, we conducted a theoretical analysis to determine the extent to which angular deviations could compromise the perception of the occlusal surface as a plane. In further sequence, clinical data and theoretically drawn assumptions were used for mechanical simulations as a proof.

During clinical dental examination, various static and dynamic orthodontic parameters such as OJ, UJ, incisor CO, LETS, DIM, smile, or frown can be assessed. Congenital malocclusion of maxillary incisor teeth that protrude labially to mandibular

incisor teeth in the horizontal plane is termed overjet (OJ), while loss of occlusal contact and vertical tooth overlap is termed overbite or "parrot mouth" (Dixon et al., 2022). Similarly, labial protrusion of mandibular incisor teeth is referred to as underjet (UJ) and with vertical overlap as underbite or "monkey mouth" (Rawlinson and Earley, 2013; Dixon et al., 2022). Physiological motion dynamics, however, also need consideration when assessing these orthodontic parameters. It is known that the mandibular position relative to maxilla changes during different head positions and that there is also protrusion/retrusion mobility of the mandible during chewing (Simhofer et al., 2011; Carmalt et al., 2003; Griffin, 2013). We clinically observed that most horses included in our study exhibited a higher degree of incisor occlusal surface superimposition with lowered head position as if grazing, compared to when their head was elevated, and the mandible was retracting due to assumed passive muscle pull. It is welldescribed in humans that mandibular position changes with head position and is determined by muscle tone and inherent muscle

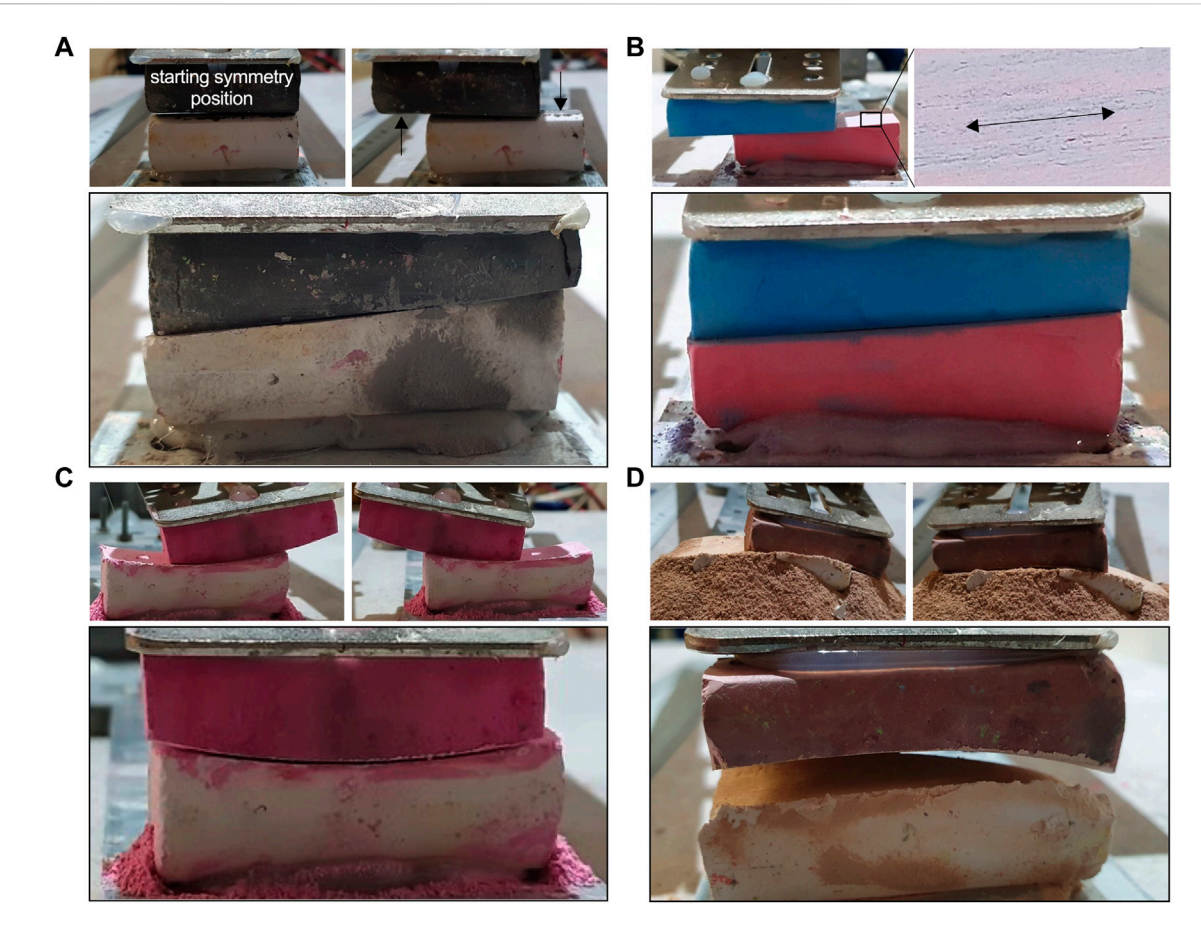


FIGURE 8

Mechanical malocclusion simulation. (A, B) Diagonal malocclusion representing asymmetric latero-lateral motion pattern no. 1 (A) and asymmetric pattern no. 2 (B). Here the movement is limited by the latero-lateral symmetry position and the left point of LETS. After 20 k cycles, a clear DIM becomes visible. The black arrows in (A) mark the regions with reduced abrasion due to lack of contact. Despite a DIM, the occlusal surface remains largely flat and with a latero-lateral oriented wear pattern. (C) Smile malocclusion, (D) frown malocclusion.

visco-elasticity (Woda et al., 2001). This further leads to the assumption that state of muscle relaxation may differently affect mandibular position in sedated animals. At least to reduce head position influence on a minimum, we standardized it for orthodontic measurements. Nevertheless, describing the dynamic range of mandibular motion during incisor occlusion remains a challenge in horses. Thus, recorded OJ and UJ in our study are still an approximation, which we conservatively estimated upward in theoretical computations of mandibular pitch and roll during incisor occlusion and subsequent mechanical simulations. In the reported head position, OJ was much more frequent (52.9%) as UJ (0.8%), revealing values of 4.2 ± 2.5 mm (range: 0–20 mm) and 2.4 ± 0.5 mm (range: 0-3 mm), respectively. Domanska-Kruppa et al. (2018); Domanska-Kruppa et al. (2019) radiographically measured an OJ in 2% of 650 Warmblood foals ranging from 4 to 8 mm, but with the head fixed in a flexed position (Domanska-Kruppa et al., 2018; Domanska-Kruppa et al., 2019). Reporting an OJ prevalence of 51% in Quarter Horse foals in a head position comparable to Domanska-Kruppa et al. (2018) and Omura et al. (2015) measured mean OJ ranging from 0.5 to 1.74 mm in different age groups (Omura et al., 2015). Although reporting a similar prevalence to that observed in our study, OJ amplitude was smaller. Elevating the head to a position like that used in our study would have potentially led to higher OJ values in other studies. Gift et al. (1992) reported even higher OJ values ranging from 7.5 to 30 mm, but only evaluated horses referred due to incisor malocclusion. Dynamic protrusion/retrusion mandibular range motion during chewing was reported to be 8.8 ± 2.2 mm in larger horses (Bonin et al., 2007; Simhofer et al., 2011). This range we assumed is within the range of incisor occlusion as is our measured range of OJ upon head elevation. To even better approximate mandibular protrusion and retrusion under incisor occlusion, it is desirable in future studies to gather individual OJ or UJ in different standardized head positions.

Incisor separation upon jaw deflection in LETS measurement is a good indicator of dynamic occlusion loss in incisor teeth area and can be used adapted to head dimensions in occlusion simulation experiments. Its determination should be part of routine dental examination as it indicates the degree of cheek tooth occlusion (Easley et al., 2011b). Published mean LETS range from 11.7 to 12.3 mm (Rucker, 2002; Rucker, 2004; Pimentel and Zoppa AL do, 2014), whereas LETS in miniature horses and ponies were reported to be 5–6 mm (Rucker, 2008). Our measured population-wide mean was 14.0 ± 4.3 mm (left) and 12.8 ± 4 mm (right). The LETS measured in ponies was slightly higher in our study with

 $8.6 \pm 1.9 \, \text{mm}$ (left) and $9.9 \pm 2.8 \, \text{mm}$ (right). This may be due to reference to miniature pony breeds in literature. However, when measuring LETS, potential incisor center offset (CO) due to rostral bony or dental asymmetries needs to be considered. Such asymmetries may cause TMJ "neutral" position not to be associated with centered incisor occlusion and TMJ range of motion would likely be unaffected. However, symmetry of bilateral laterotrusion and thus incisor occlusion during mastication would be affected, resulting in development of malocclusion wear patterns such as DIM. The latter malocclusion was developed in our simulations upon mimicking asymmetric laterotrusion under incisor occlusion. If the degree of DIM in horses correlates with the extension of LETS, asymmetry needs to be further investigated on standardized clinical data.

In the theoretical description and calculations of TMJ movements, we have averted from the medical directional specifications "rostral-caudal-dorsal-ventral" since these describe possible mandibular movements in relation to the maxilla inaccurately. By using a segment coordinate system—commonly used in biomechanics (Wittenburg, 2007)—we were able to specify the directional information of the mandibular movement under incisor occlusion at the level of the occlusal surface plane accordingly. In our theoretical calculations of any possible deviations of the incisor occlusal surface from a plane, the focus was on a reasonable estimation of movement parameters causing angular deviation. The literature on dynamic masticatory biomechanics in horses is scarce (Huthmann et al., 2009; Neto et al., 2018). We therefore had to incorporate estimates of head dimensions through our own morphometric analyses on CT data sets and skull specimen. In doing so, we have always made significant upward estimates. Despite these findings, angular deviations calculated during incisor occlusion (mandibular pitch and roll) are so small that they do not affect visual perception and thus maintenance of occlusal surfaces as a plane. With a more realistic estimation of the underlying movement directions and distances, even significantly smaller angles are to be expected. As feed intake is the major motivator for chewing, it is reasonable to assume that a significant portion of tooth wear occurs not through tooth-to-tooth friction alone, but rather in conjunction with the presence of feed. The latter creates a gap between incisor and cheek tooth occlusal surfaces, resulting in additional angular changes that are hard to model. However, when incisor occlusal surfaces are subjected to chewing pressure, the distance between them should only be a few millimeters and would be mathematically assessed as the d_{LPR} component of mandibular AH movement. Consequently, only a small angular alteration in the sub-angle degree range can be anticipated here as well. In the worst case, this angle alteration could add up to the calculated angular change, $\Delta \alpha$, under protrusion. Using CT-based cephalometrics in horses, Listmann et al. (2017) had shown in addition that mandibular incisor teeth under centered occlusion feature slightly steeper sagittal occlusal surface angles; mandibular = 38-44.9 angle deg.; maxillary = 32.7-35.6 angle deg. Accordingly, it can be assumed that even higher $\Delta\alpha$ than that modeled in our study (WBL = 1.16 angle deg. and pony = 0.82 angle deg.), and in addition to higher $\Delta\alpha$ due to feed intake, does not interfere with the maintenance of a flat occlusal surface plane. As a figurative representation, we found it helpful to visualize material processing with the aid of a file: only when the file is guided over a workpiece without tilting can a flat surface be achieved. When introducing high mandibular roll $(\Delta \gamma)$ to our mechanical simulations, curvature malocclusions smile and frown are observed.

The mechanical simulator used is a very simplified representation of equine dentition. In human dental research, chewing simulators are often used for wear and fatigue tests of filling materials (Soriano-Valero et al., 2020). Several authors use a software-controlled simulator with two motor-driven axes that can mimic different motion patterns (Jensen and Abbott, 2007; Heintze et al., 2011; Rues et al., 2011; Shahin et al., 2014). Unlike a real horse, the simulator in this study has two axes of rotation, namely, the actual servo axis and the attachment point on the aluminum rail. The latter non-driven connection between the servo arm and the aluminum splint represents the TMJ hinge movement. This double joint nevertheless reproduces the SAP+/SAP- mobility with good precision. In the simulations, occlusion was maintained by gravity. All movements were thus tooth-guided, meaning under occlusion and guided by the shape of the occlusal surface. The servo drive made it possible to describe SAP+/SAP- sliding of the mandibular AH. In the horse, this movement is muscle-driven, while in the simulator the servo motor actively adjusts the AH position. Only when attempting to simulate mandibular roll around the SAP axis does a difference in the cause of AH SAP⊥ motion components occur. In the simulator, this SAP portion arose due the servo starting position choice. In the real horse, we assume the possibility of lateral movement (side shift) of the mandibular AH in addition, which, however, cannot be assessed with the current simulator in its full extent. Nevertheless, mandibular protrusion and retrusion movement in our simulator is performed on a circle segment and always comes in combination with a moderate SAP

movement component as presented in Table 1. This is in alignment with our assumptions regarding TMJ movement in a horse.

Due to its rather simple construction, we used the chalk simulator only for qualitative confirmation of theoretical considerations. The focus was on achieving the planar shape of the occlusal surface plane. In addition, we were able to provide TMJ movement indicators for the development of malocclusions by deliberately changing movement patterns. In equine research, Karme et al. (2016) mounted single real maxillary and mandibular cheek teeth in a chewing machine and compared microwear and gross wear characteristics after 100,000 chewing cycles between different diets and pure attrition. The chalk bars representing incisor teeth in our study have a hardness between 1 and 2 on the Mohs hardness scale, ranging from 1 to 10. Enamel is the hardest dental tissue and ranges between 4.5 and 5.0 on the Mohs scale (Baker et al., 1959). As a result, the experimental formation of the surface shape by attrition on the occlusal surfaces in our study could already be observed after a significantly lower number of movement cycles in the order of 10 k cycles and under lower occlusal pressure of approx. 1.5 N. Englisch et al. (2018) speculated that less masticatory forces act on the incisor compared to the cheek teeth because they detected a shorter pulp to occlusal surface distance in incisor teeth. The chalk bars have the shape of a cuboid, while real arcades are more of a crescent shape. In addition, the hardness distribution in the chalk is largely homogeneous, while incisor teeth in the horse have hard enamel areas and softer dentin and cementum areas (Du Toit et al., 2008; Erickson et al., 2014). We assume, however, that the difference in shape and structure has only a marginal influence on the forming surface shape.

Horses with a DIM show a tilted incisor occlusal surface plane when viewed from the front (Rucker, 2004). Most DIMs are associated with deformation of the maxilla or incisive bone (Earley, 2011). It has also been assumed that chewing in only one direction can lead to DIM (Dixon and Dacre, 2005). The prerequisite is long-term asymmetrical mastication. In our study, a DIM could be provoked by asymmetrical laterotrusion movements, which coincides with the experience from the clinical field. Here, too, DIM is frequently reported in combination with unilateral mastication due to dental disease in the then spared cheek tooth arcade. This is consistent with the literature where skeletal deviation or asymmetry is associated with DIM (Dixon, 2002; DeLorey, 2007). Despite DIM formation, the occlusal surface hardly deviates from a flat inclined plane. Proven in our simulations, DIM formation is thus due to changed wear of the arcades resulting from asymmetric laterotrusion movements.

Equids with pronounced anisognathia tend to develop dorsal curvature of the incisor teeth (Du Toit et al., 2009). We demonstrated that a rotation of the jaw around an SAP+/SAP- axis in combination with a laterotrusion movement of the incisor teeth have the potential to explain the development of a smile or frown malocclusion. Both differ in whether the rotation and the latero-lateral movement are concurrent or opposed. In a real horse, the rotation of the jaw may be caused by the shape of the maxillary articulation area in combination with transversal mandibular AH movements. The extend of cheek tooth anisognathia could also influence the anatomically permissible degree of jaw rotation, as in pronounced anisognathia, there may be later rotation delimiting cheek tooth contact.

There is little evidence on the normal occlusal state and range in equine incisor teeth. It is important, as we did in this study here, to perform static and dynamic orthodontic measurements in a wide set of horses of different oro-dental states. We were particularly struck by lack of knowledge about the exact course of lateral jaw excursion during the chewing process as described in the introduction. Here, different explanatory models are in contradiction. On the other hand, little is known about associated TMJ movements. In high similarity to the well-understood human masticatory process, we favor laterotrusion pattern no. 2, i.e., a lateral deflection over a rotating working-side mandibular AH with simultaneous sliding of the balancing-side mandibular AH in SAP+ direction. Though, experimental confirmation would be desirable here.

Conclusion

The study's comprehensive findings encompassing clinical assessments, theoretical calculations, and mechanical simulations contribute to the existing body of evidence regarding orthodontic measurements, confirming the perception of the incisor occlusal surface as a plane. The clinical part provides confident delineation of the range of potential mandibular movement under incisor occlusion, leveraging LETS, and OJ or UJ measurements. This delineation holds profound implications for theoretical appraisal of dynamic angular changes in the mandible and TMJs as well as biomechanical simulations. Intriguingly, our study introduces a novel perspective by introducing the segmental coordinate system to the equine head, shedding fresh light on the intricacies behind the formation of a level occlusal surface plane. By amalgamating analyses of possible laterotrusion movement patterns no. 1 and no. 2, we systematically

ascertain angular deviations. The insights from this study serve as a foundational cornerstone, facilitating further explorations and potentially leading to invaluable advancements in dental care of horses through the application of orthodontic measurements.

We hope that our study will contribute to early identification of further dentition abnormalities and allow timely intervention and prevention. Overall, it could support clinicians in diagnosing and managing dental conditions more effectively by applying more targeted and individualized treatment strategies for the sake of an improved oral health and wellbeing of the horse.

Study limitations

First, our modeling relies on physiologic horse dentition and does not incorporate variables such as cheek tooth pathologies, dental treatment, and feed consistency, which may influence the mandibular range of motion and incisor attrition. Second, the qualitative results obtained from mechanical simulations limit our ability to draw quantitative conclusions due to the system's simplicity and expected deviations from real-world scenarios. Simulator design mainly limits the accurate representation of side shift movement. These limitations should be taken into consideration when interpreting the findings of this study.

Data availability statement

The raw data supporting the conclusions of this article will be made available by the authors, without undue reservation.

Ethics statement

The requirement of ethical approval was waived by Ethics committees of the University of Veterinary Medicine Vienna, Austria, for the studies involving animals because according to the national legislation, ethical review and approval were waived for this study as all investigated data were obtained for clinical reasons not related to this study. The horse owners gave their consent after being adequately informed about the care, diagnostic, and treatment options for their animals. The use of achieved diagnostic material complied with the guidelines specified by the local ethics committees of the University of Veterinary Medicine Vienna, Austria, to be based on the regulations of good scientific practice. The studies were conducted in accordance with the local legislation and institutional requirements. Written informed consent was obtained from the owners for the participation of their animals in this study.

Author contributions

TS, MN, and SK conceived the presented idea and designed the study with the help of BH and CP. SK performed all orodental examinations leading to the embraced clinical static and dynamic orthodontic data. SK and BH analyzed and interpreted orthodontic data. TS did all theoretical calculations to describe TMJ dynamics, built the mechanical simulator, and performed all associated measurements. All authors contributed to the interpretation of

the results. SK prepared all figures with input from TS and BH. TS prepared all tables. SK and TS supervised the work. TS, BH, and SK prepared the original draft. CP, MN, and MK reviewed and edited the original draft. All authors contributed to the article and approved the submitted version.

Funding

Open access funding provided by Vetmeduni, Vienna, Austria.

Acknowledgments

We would like to thank Prof. Carsten Staszyk, Justus Liebig University in Giessen, for the opportunity to take and use photographic images of the anatomical specimen shown in Figure 2C. Some raw data that form the basis for evaluation of static and dynamic orthodontic parameters were published as a Conflict of interest

of SK and BH.

The authors declare that the research was conducted in the absence of any commercial or financial relationships that could be construed as a potential conflict of interest.

diploma thesis at Vetmeduni, Vienna (2022) under the supervision

Publisher's note

All claims expressed in this article are solely those of the authors and do not necessarily represent those of their affiliated organizations, or those of the publisher, the editors, and the reviewers. Any product that may be evaluated in this article, or claim that may be made by its manufacturer, is not guaranteed or endorsed by the publisher.

References

Baker, G., Jones, L. H. P., and Wardrop, I. D. (1959). Cause of wear in sheeps' teeth. $Nature\ 184,\ 1583-1584.$ doi:10.1038/1841583b0

Baker, G. J. (2005). "Dental physiology," in *Equine dentistry*. Editor J. Easley (Amsterdam, Netherlands: Elsevier), 49–54.

Bennett, N. G. (1908). A contribution to the study of the movements of the mandible. *Proc. R. Soc. Med.* 1, 79–98. doi:10.1177/003591570800100813

Bonin, S. J., Clayton, H. M., Lanovaz, J. L., and Johnson, T. J. (2006). Kinematics of the equine temporomandibular joint. Am. J. Vet. Res. 67, 423–428. doi:10.2460/ajvr.67.3.423

Bonin, S. J., Clayton, H. M., Lanovaz, J. L., and Johnston, T. (2007). Comparison of mandibular motion in horses chewing hay and pellets. *Equine Vet. J.* 39 (3), 258–262. doi:10.2746/042516407X157792

Carmalt, J. L., Townsend, H. G. G., and Allen, A. L. (2003). Effect of dental floating on the rostrocaudal mobility of the mandible of horses. *J. Am. Vet. Med. Assoc.* 223 (5), 666–669. doi:10.2460/javma.2003.223.666

Collinson, M. (1994). "Food processing and digestibility in horses (*Equus caballus*),". BSc Dissertation (Melbourne, Australia: Monash University).

DeLorey, M. S. (2007). A retrospective evaluation of 204 diagonal incisor malocclusion corrections in the horse. *J. Vet. Dent.* 24 (3), 145–149. doi:10.1177/089875640702400302

Dixon, P. M., and Dacre, I. (2005). A review of equine dental disorders. *Veterinary J.* 169 (2), 165–187. doi:10.1016/j.tvjl.2004.03.022

Dixon, P. M., and du Toit, N. (2011). "Dental anatomy," in *Equine dentistry*. Editors J. Easley, P. M. Dixon, and S. James (Philadelphia, PA, USA: Saunders Elsevier), 51–76.

Dixon, P. M. "The gross, histological, and ultrastructural anatomy of equine teeth and their relationship to disease," in Proceedings of the Annual Convention of the AAEP, San Diego, CA, USA, December 2002, 421–437.

Dixon, P. M., and Vlaminck, L. (2022). "Abnormalities of craniofacial development and of dental development and eruption," in *Equine dentistry and maxillofacial surgery*. Editors J. Easley, P. M. Dixon, and N. du Toit (Newcastle, UK: Cambridge Scholars Publishing), 141–160.

Domanska-Kruppa, N., Venner, M., and Bienert-Zeit, A. (2019). Cephalometric study of the overjet development in Warmblood foals. *Front. Vet. Sci.* 6, 431. doi:10.3389/fvets. 2019.00431

Domanska-Kruppa, N., Venner, M., and Bienert-Zeit, A. (2018). Study of the relationship between overjet development and some skull bone measurements in Warmblood foals. *Veterinary Rec.* 183 (11), 353. doi:10.1136/vr.104364

Du Toit, N., Bezensek, B., and Dixon, P. M. (2008). Comparison of the microhardness of enamel, primary and regular secondary dentine of the incisors of donkeys and horses. *Veterinary Rec.* 162 (9), 272–275. doi:10.1136/vr.162.9.272

Du Toit, N., Burden, F. A., and Dixon, P. M. (2009). Clinical dental examinations of 357 donkeys in the UK. Part 1: prevalence of dental disorders. *Equine Vet. J.* 41 (4), 390–394. doi:10.2746/042516409X368912

Earley, E. "Skeletal abnormalities in the equine skull," in Proceedings of the Focus on Dentistry AAEP, Albuquerque, NM, USA, January 2011, 131–133.

Easley, J. (2011a). "Basic equine orthodontics," in *Equine dentistry*. Editors J. Easley, P. M. Dixon, and J. Schumacher (Philadelphia, PA, USA: Saunders Elsevier), 249–266.

Easley, J., Dixon Padraic, M., and James, S. (2011b). "A glossary of equine dental terminology," in *Equine dentistry*. Editors J. Easley, P. M. Dixon, and J. Schumacher (Philadelphia, PA, USA: Saunders Elsevier), 328–346.

Englisch, L. M., Rott, P., Lüpke, M., Seifert, H., and Staszyk, C. (2018). Anatomy of equine incisors: pulp horns and subocclusal dentine thickness. *Equine Vet. J.* 50 (6), 854–860. doi:10.1111/evj.12841

Erickson, K. L., Krick, B. A., Hamilton, M., Bourne, G. R., Norell, M. A., Lilleodden, E., et al. (2014). Complex dental structure and wear biomechanics in hadrosaurid dinosaurs. *Hist. Biol.* 26 (6), 98–101. doi:10.1126/science.1224495

Gift, L. J., DeBowes, R. M., Clem, M. F., Rashmir-Raven, A., and Nyrop, K. A. (1992). Brachygnathia in horses: 20 cases (1979-1989). $J.\ Am.\ Vet.\ Med.\ Assoc.\ 200\ (5), 715-719.$

Griffin, C. (2013). The gold standard of dental care. Veterinary Clin. N. Am. Equine Pract. 29 (2), 487–504. doi:10.1016/j.cveq.2013.04.004

Heintze, S. D., Albrecht, T., Cavalleri, A., and Steiner, M. (2011). A new method to test the fracture probability of all-ceramic crowns with a dual-axis chewing simulator. *Dent. Mater.* 27 (2), e10–e19. doi:10.1016/j.dental.2010.09.004

Hongo, A., and Akimoto, M. (2003). The role of incisors in selective grazing by cattle and horses. J. Agric. Sci. 140 (4), 469–477. doi:10.1017/S0021859603003083

Huthmann, S., Staszyk, C., Jacob, H. G., Rohn, K., and Gasse, H. (2009). Biomechanical evaluation of the equine masticatory action: calculation of the masticatory forces occurring on the cheek tooth battery. *J. Biomech.* 42 (1), 67–70. doi:10.1016/j.jbiomech.2008.09.040

Imfeld, T. (1996). Dental erosion. Definition, classification and links. *Eur. J. Oral Sci.* 104 (2), 151–155. doi:10.1111/j.1600-0722.1996.tb00063.x

Jensen, A. L., and Abbott, P. V. (2007). Experimental model: dye penetration of extensive interim restorations used during endodontic treatment while under load in a multiple axis chewing simulator. *J. Endod.* 33, 1243–1246. doi:10.1016/j.joen.2007. 06.014

Karme, A., Rannikko, J., Kallonen, A., Clauss, M., and Fortelius, M. (2016). Mechanical modelling of tooth wear. *J. R. Soc. Interface* 13 (120), 20160399. doi:10. 1098/rsif.2016.0399

Kau, S., Failing, K., and Staszyk, C. (2020). Computed tomography (CT)-Assisted 3D cephalometry in horses: interincisal angulation of clinical crowns. *Front. Vet. Sci.* 7, 434. doi:10.3389/fvets.2020.00434

Koolstra, J. H. (2002). Dynamics of the human masticatory system. Crit. Rev. Oral Biol. Med. 13 (4), 366–376. doi:10.1177/154411130201300406

Kunz, J. R., Granella, M. C. S., Mendes, R. P., Müller, T. R., Kau, S., and Fonteque, J. H. (2020). High prevalence of orodental disorders in South Brazilian cart horses: walking a tightrope between animal welfare and socioeconomic inevitability. *J. Vet. Dent.* 37 (3), 149–158. doi:10.1177/0898756420968306

Lambrechts, P., Debels, E., Van Landuyt, K., Peumans, M., and Van Meerbeek, B. (2006). How to simulate wear? Overview of existing methods. *Dent. Mater.* 22 (8), 693–701. doi:10.1016/j.dental.2006.02.004

Limone, L. (2022). "General clinical, oral and dental examination," in *Equine dentistry and maxillofacial surgery*. Editors J. Easley, P. Dixon, and N. du Toit (Newcastle, UK: Cambridge Scholars Publishing), 302–326.

Listmann, L., Schrock, P., Failing, K., and Staszyk, C. (2017). Occlusal angles of equine incisors. *J. Vet. Dent.* 34 (4), 259–267. doi:10.1177/0898756417739465

Muylle, S., Simoens, P., Verbeeck, R., Ysebaert, M. T., and Lauwers, H. (1999). Dental wear in horses in relation to the microhardness of enamel and dentine. *Veterinary Rec.* 144 (20), 558–561. doi:10.1136/vr.144.20.558

Neto, A. O. P., Leite, C. T., Duarte, C. A., Dias, D. P. M., Döwich, G., Neto, A. Q., et al. (2018). Biomechanical analysis of the masticatory movement before and after adjusting dental occlusion in equine. *Arq. Bras. Med. Vet. Zootec.* 70 (1), 6–12. doi:10.1590/1678-4162-9491

Omura, C. M., Drumond, B., Júnior, J. L. R., Coelho, C. S., and Gioso, M. A. (2015). Measurement of incisor overjet and physiological diastemata parameters in quarter horse foals. *J. Vet. Dent.* 32 (3), 173–175. doi:10.1177/089875641503200304

Pellachin, M. "Objective measurements of occlusal angles," in Proceedings of the 11 IGFP-Conference, Niedernhausen, Germany, March 2013, 45–57.

Pimentel, L. F. R., and Zoppa al do, V. (2014). Analysis of the relationship between occlusal and clinical parameters and the need for incisor reduction in confined horses - a retrospective study. *Ciência Rural.* 44 (11), 2052–2057. doi:10.1590/0103-8478cr20130955

Preiskel, H. W., and Goldstein, G. (2021). The clinical significance of immediate mandibular lateral translation: critically appraised topic (CAT). *J. Prosthodont.* 30 (1), 64–66. doi:10.1111/jopr.13317

Rawlinson, J. T., and Earley, E. (2013). Advances in the treatment of diseased equine incisor and canine teeth. *Veterinary Clin. N. Am. Equine Pract.* 29 (2), 411–440. doi:10. 1016/j.cveq.2013.04.005

Rucker, B. A. (2008). "Excursion to molar contact," in Am assoc eq pract dental wet lab notes (Berlin, Germany: Springer), 31–37.

Rucker, B. A. (2004). Equine cheek teeth angle of occlusion: how to calculate and clinical use for incisor shortening. *Equine Vet. Educ.* 16 (3), 137–142. doi:10.1111/j. 2042-3292.2004.tb00284.x

Rucker, B. A. "Utilizing cheek teeth angle of occlusion to determine length of incisor shortening," in Proceedings of the Annual Convention of the AAEP, Orlando, FL, USA, December 2002, 448–452.

Rues, S., Huber, G., Rammelsberg, P., and Stober, T. (2011). Effect of impact velocity and specimen stiffness on contact forces in a weight-controlled chewing simulator. Dent. Mater. 27 (12), 1267–1272. doi:10.1016/j.dental.2011.09.007

Shahin, R., Tannous, F., and Kern, M. (2014). Inlay-retained cantilever fixed dental prostheses to substitute a single premolar: impact of zirconia framework design after dynamic loading. *Eur. J. Oral Sci.* 122 (4), 310–316. doi:10.1111/eos.12134

Schrock, P., Lüpke, M., Seifert, H., and Staszyk, C. (2013). Finite element analysis of equine incisor teeth. Part 2: investigation of stresses and strain energy densities in the periodontal ligament and surrounding bone during tooth movement. *Veterinary J.* 198 (3), 590–598. doi:10.1016/j.tvjl.2013.10.010

Simhofer, H., Niederl, M., Anen, C., Rijkenhuizen, A., and Peham, C. (2011). Kinematic analysis of equine masticatory movements: comparison before and after routine dental treatment. *Veterinary J.* 190 (1), 49–54. doi:10.1016/j.tvjl.2010. 09.014

Smuts, G. L. (1974). Age determination in burchell's zebra (Equus burchell! Ant/ Quorum) from the kruger national park. South African Journal of Wildlife Research 4 (2), 103–115. doi:10.520/AJA03794369_2679

Soriano-Valero, S., Román-Rodriguez, J., Agustín-Panadero, R., Bellot-Arcís, C., Fons-Font, A., and Fernández-Estevan, L. (2020). Systematic review of chewing simulators: reality and reproducibility of *in vitro* studies. *J. Clin. Exp. Dent.* 12, e1189–e1195. doi:10.4317/jced.57279

Staszyk, C., and Carmalt, J. L. (2022). "Equine mastication: morphological, functional biomechanical adaptions," in *Equine dentistry and maxillofacial surgery*. Editors J. Easley, P. Dixon, and N. du Toit (Newcastle, UK: Cambridge Scholars Publishing), 99–110.

Staszyk, C., Lehmann, F., Bienert, A., Ludwig, K., and Gasse, H. (2006a). Measurement of masticatory forces in the horse. *Pferdeheilkunde* 22 (1), 12–16. doi:10.21836/pem20060102

Staszyk, C., Wulff, W., Jacob, H. G., and Gasse, H. (2006b). Collagen fiber architecture of the periodontal ligament in equine cheek teeth. *J. Vet. Dent.* 23 (3), 143–147. doi:10. 1177/089875640602300303

Sterkenburgh, T., Schulz-Kornas, E., Nowak, M., and Staszyk, C. (2022). A computerized simulation of the occlusal surface in equine cheek teeth: A simplified model. *Front. Vet. Sci.* 8, 789133. doi:10.3389/fvets.2021.789133

Taylor, W. T. T., Bayarsaikhan, J., Tuvshinjargal, T., Bender, S., Tromp, M., Clark, J., et al. (2018). Origins of equine dentistry. *Proc. Natl. Acad. Sci. USA.* 115 (29), E6707–E6715. doi:10.1073/pnas.1721189115

Tremaine, H. (1997). Dental care in horses. Pract 19 (4), 186–199. doi:10.1136/inpract.19.4.186

Weinert, J. R., Werner, J., and Williams, C. A. (2020). Validation and implementation of an automated chew sensor-based remote monitoring device as tool for equine grazing research. *J. Equine Vet. Sci.* 88, 102971. doi:10.1016/j.jevs.2020.102971

Wittenburg, J. (2007). "Rigid body kinematics," in *Dynamics of multibody systems* (Berlin, Germany: Springer), 9–36.

Woda, A., Pionchon, P., and Palla, S. (2001). Regulation of mandibular postures: mechanisms and clinical implications. *Crit. Rev. Oral Biol. Med.* 12 (2), 166–178. doi:10. 1177/10454411010120020601